Available online at www.sciencedirect.com
ScienceDirect
Colloids and Surfaces A: Physicochem. Eng. Aspects 301 (2007) 63–68
COLLOIDS AND SURFACES A
www.elsevier.com/locate/colsurfa

The dielectric spectrum and the electrorheological effect in suspensions of varying conductivity Part 1. Modeling of the dielectric spectrum

L. Rejón [a,*], F. Bautista [b], O. Manero [c]

[a] *Gerencia de Materiales y Procesos Químicos, Instituto de Investigaciones Eléctricas, Calle Reforma 113, Colonia Palmira, Cuernavaca, Mor. 62490, Mexico*
[b] *Departamento de Física, Universidad de Guadalajara, Blvd. M. García Barragán 1451, Guadalajara, Jal. 44430, Mexico*
[c] *Instituto de Investigaciones en Materiales, Universidad Nacional Autónoma de México, A.P. 70-360 México, D.F., Mexico*

Received 16 June 2006; received in revised form 30 November 2006; accepted 4 December 2006
Available online 8 December 2006

Abstract

The dielectric behavior of electrorheological (ER) suspensions composed of non-colloidal silica gel particles of irregular shape and liquids with varying conductivity is examined in this work. The dielectric properties of the suspensions are analyzed in the diluted and semi-concentrated regimes at different frequencies maintaining the electric field constant. Primarily, the dielectric behavior is studied with particular attention to the dependence of the dielectric relaxation process on particle concentration and their relation with the conductive behavior.

The dielectric spectrum is analyzed with Maxwell–Wagner interfacial polarization model in the low frequency region and with the Debye model at moderate frequencies. A non-localized diffusion process (or ideal conduction) is considered to analyze the dielectric spectrum in more conductive suspensions. Since a strong correlation exists between the ER activity of a suspension and its dielectric spectrum, the modeling of the dielectric spectrum provides understanding of the polarization processes which induce the ER effect studied in Part 2.

Keywords: Electrorheology; Dielectric relaxation; Conductivity; Suspensions

1. Introduction

Electrorheological (ER) suspensions are materials that drastically change their rheological behavior upon application of an electric field. Generally, this change is associated to an increase in the stress when an electric field is applied perpendicular to the direction of shearing. This increase in the stress is associated to the fibrous structure formation caused by the polarization forces. Several mechanisms have been proposed to explain the origin of the ER response, among them, particle polarization, electric double layers, interfacial polarization, conduction and dielectric loss. In this regard, the dielectric spectrum of the suspension greatly influences their ER response, in as much as the presence of dielectric relaxation phenomena leads to the redistribution of charges at the interface between the particles and the surrounded field. Particles aggregate provided that a certain relation between the ratio of the particle-to-suspending fluid dielectric constants and that of the conductances is satisfied. Consequently, the ER response is influenced by the mismatch between the relative permittivities of the solid and liquid phase in the suspension [1]. A great deal of work has been done in recent years to establish the role of the mismatch conductivity in ER suspensions [2].

The relative permittivity (ε') of a homogeneous material is related with the capacity of this material to polarize in the presence of the electric field. Every type of dielectric loss is related to the charge motion and the energy involved in this process. The total polarization is the sum of several contributions: electronic, atomic, Debye (related to the orientation of dipoles) and interfacial polarization (the Maxwell–Wagner polarization). The Debye and interfacial polarizations are located in the low-frequency range of the spectrum, while the electronic and atomic polarizations are fast polarizations, appearing at high frequencies. From studies on the influence of particle conductivity and surface properties of the particles on the ER effect, it was con-

* Corresponding author. Tel.: +52 777 3623831; fax: +52 777 3623832.
E-mail address: lrejon@iie.org.mx (L. Rejón).

0927-7757/$ – see front matter © 2006 Elsevier B.V. All rights reserved.
doi:10.1016/j.colsurfa.2006.12.022

cluded [3] that the interfacial polarization contributes to the ER effect. Moreover, in homogeneous two-component ER systems, the interfacial polarization is also found to be responsible for the ER effect [4].

The dielectric loss factor is related to both energy dissipation and dielectric polarization rate, estimated from the maximum of the loss peak [3,4]. It has been reported [5–8] that a fluid with good ER effect must have a relaxation frequency from 100 to 10^5 Hz.

Summarizing, the interfacial polarization of the particles affects the electric-field induced-aggregation in electrorheological fluids. Hence, a correlation exists between the ER activity of a suspension and its dielectric spectrum.

In Part 1 of this series, we study the effect of the liquid phase properties (conductivity and relative permittivity) and concentration of the particles on the dielectric behavior of the ER suspensions. Dielectric data are described using the interfacial polarization (Maxwell–Wagner) and Debye models. Their relation with the macroscopic rheological behavior is examined in Part 2.

2. Experimental part

2.1. Preparation of the electrorheological suspensions

The ER suspensions employed in this study were prepared using suspensions of silica particles of irregular form (Merck 60, 0.015–0.040 mm) of approximately 22.1 μm in average size in silicon oil, dioctyl phthalate and tricresyl phosphate. Solid volume fractions considered are 0.03 and 0.16. The blend was prepared in a Cowles-type mixer during 10 min at 3000 rpm. Table 1 contains a summary of the corresponding viscosity and dielectric properties of particles and fluids. The ER suspensions were placed in a vacuum chamber to extract the air bubbles previous to dielectric measurements.

2.2. Dielectric characterization

Dielectric measurements were performed in a Dupont (DEA 2970) dielectric analyzer. Experimental conditions covered a frequency range of 0.1–100 000 Hz, 1 V amplitude at 30 °C. The relative permittivity of the silica particle ε_p was estimated from that of the suspension by a volume average calculation [9] given by the equation

$$\varepsilon = \varepsilon_p\phi + (1-\phi)\varepsilon_L \quad (1)$$

where ε and ϕ are the relative permittivity and volume fraction of the suspension and ε_L the relative permittivity of the fluid. The impedance (Z^*) and modulus (M^*) of the suspensions were calculated through the field transformations:

$$Z' = \frac{M''}{\omega C_0} \quad (2)$$

$$Z'' = \frac{M'}{\omega C_0} \quad (3)$$

$$M' = \frac{\varepsilon'}{\varepsilon'^2 + \varepsilon''^2} \quad (4)$$

$$M'' = \frac{\varepsilon''}{\varepsilon'^2 + \varepsilon''^2} \quad (5)$$

where C_0 is the vacuum capacitance, ω is the frequency and the complex nomenclature is implied.

3. Results and discussion

3.1. Dielectric properties

The combination of impedance and modulus spectroscopy has been showed as a useful technique in the analysis of dielectric data, since they display complementary information. Both bulk and interfacial impedances are separated in a simple and convenient form. Differences occur because the two methods apply different weighting schemes to the experimental data. In the modulus representation, the height of each peak is proportional to the inverse dielectric constant and so, information about the electrode-solution double layer and interfacial effects tend to be suppressed. A double peak in this representation is ascribed to two phases of different conductivity. On the other hand, the peak heights in the impedance spectrum are proportional to the global resistance, and so the most resistive element will dominate the spectrum. For example, the electrode effect shows up as a low frequency spike in the impedance spectrum, but it is invisible in the modulus spectrum.

The real and imaginary parts of the relative permittivity of the silicon oil–silica gel particles (0.03 volume fraction) at 30 °C are plotted in Fig. 1a and b. In Fig. 1a ε'' presents a relaxation at a frequency of 60 Hz, with relaxation time ($\tau = 0.00265$ s). This frequency corresponds to the inflection point of the relative permittivity (ε') versus frequency curve (Fig. 1b). In the low frequency range, however, the dielectric loss increases as the frequency diminishes, with inverse proportionality. This behavior closely corresponds to a superposition of two processes: a conductivity contribution corresponding to the inverse proportionality of ε'' with frequency and a relaxation process exhibiting a maximum in ε'' located at higher frequencies, the

Table 1
Characteristic of solid and liquid phases

Materials	Relative permittivity 60 Hz	Conductivity (S cm^{-1})	Viscosity (mPa s)
Silica (Merck 60, 0.015–0.040 mm)	10.9	2.0×10^{-9}	–
Silicon oil (S100)	2.40	6.8×10^{-16}	95
Dioctyl phatalate (DOP)	4.60	2.3×10^{-11}	50
Tricresyl phosphate (TCP)	6.10	1.4×10^{-9}	50

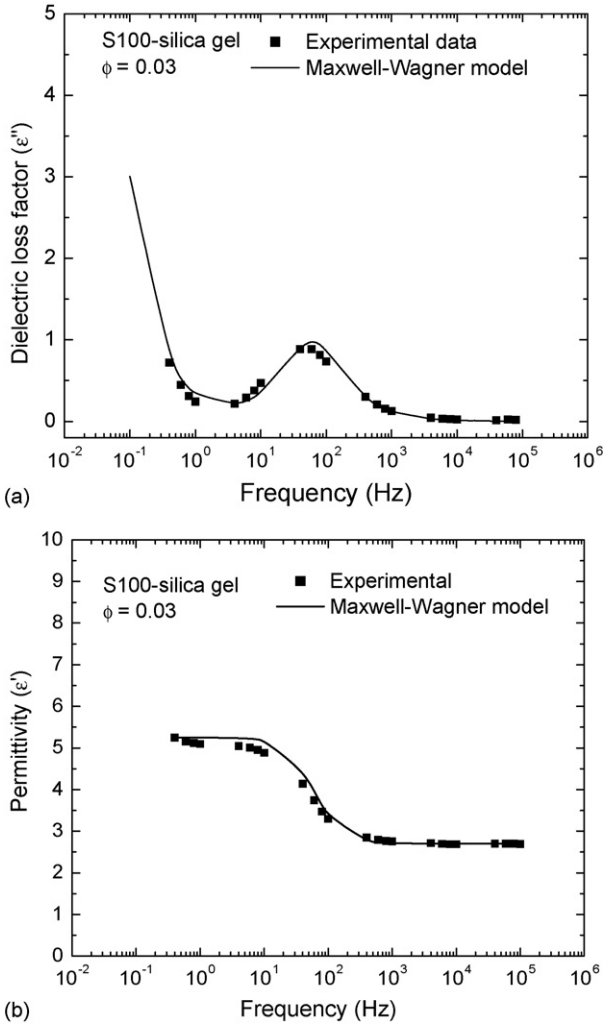

Fig. 1. (a) Dielectric loss and (b) relative permittivity, vs. frequency of silica particles in silicon oil. Experimental data and predictions of the Maxwell–Wagner polarization model (Eqs. (6) and (7)). Particle volume fraction is 0.03. Values of $\varepsilon_\infty = 2.7$, $\varepsilon_S = 5.25$, $\tau_1 = 4.8\text{E}{-4}$, $\tau_2 = 310$ and $\tau_w = 1.42$.

latter ascribed to a Debye-like relaxation process. Since the ER suspension consists of conductive particles dispersed in a dielectric medium, their polarization process should occur at the particle/oil interface [10], and hence the relaxation is located in the low frequency range [3,5]. The dominant physical process responsible for the polarization in this system (silicon oil–silica) is thus the interfacial (Maxwell–Wagner) polarization.

This process arises when the system is composed of two different phases, which differ in their permittivities or conductivities. The interfacial behavior can be modeled by a circuit consisting of two resistances (R_1 and R_2) and two capacitances (C_1 and C_2) in parallel. This can be described by the following expressions for the relative permittivity and dielectric loss:

$$\varepsilon'' = \frac{\varepsilon_\infty}{\omega\tau_w} + \frac{\Delta\varepsilon\omega\tau}{1+\omega^2\tau^2} \tag{6}$$

$$\varepsilon' = \varepsilon_\infty + \frac{\Delta\varepsilon}{1+\omega^2\tau^2} \tag{7}$$

$$\tau = \frac{\tau_1 R_2 + \tau_2 R_1}{R_1 + R_2} \tag{8}$$

$$\tau_w = \frac{\tau_1\tau_2}{\tau} \tag{9}$$

$$\tau_1 = R_1 C_1, \qquad \tau_2 = R_2 C_2 \tag{10}$$

where R_1 and C_1 are the resistance and capacitance of phase 1, τ_1 and τ_2 are time constants of the circuit representing the individual layers, the static and high frequency dielectric constants are ε_S and ε_∞, where $\Delta\varepsilon = \varepsilon_S - \varepsilon_\infty$. The interfacial polarization results from the mismatch of conductivities or permittivities of the contiguous dielectric layers. The dielectric loss exhibits an interfacial polarization term and a conductive term, the latter gives rise to the increasing loss with decreasing frequency over the lower frequency regime.

In the modulus representation, the conductive and the relaxation parts of the spectrum can be worked out from Eqs. (6) and (7). The conductive part of the spectrum can be analytically obtained by performing the limit $\omega \to 0$ of Eqs. (6) and (7) and using Eqs. (4) and (5). This gives the following approximation:

$$M'_c = \frac{\varepsilon_S^{-1}\tau_{MC}^2\omega^2}{1+\tau_{MC}^2\omega^2} \tag{11}$$

$$M''_c = \frac{\varepsilon_S^{-1}\tau_{MC}\omega}{1+\tau_{MC}^2\omega^2} \tag{12}$$

where the conductive relaxation time is given by:

$$\tau_{MC} = \left(\frac{\varepsilon_S}{\varepsilon_\infty}\right)\tau_w \tag{13}$$

The modulus peak of M'' has a magnitude of

$$M''_{c\,max} = \frac{1}{2}\varepsilon_S^{-1} \tag{14}$$

located at a frequency $\omega_{max} = \tau_{MC}^{-1}$.

The relaxation part of the spectrum corresponding to a Debye process can be expressed in terms of the modulus representation according to the following expressions:

$$M'_D = \frac{\varepsilon_S^{-1} + \varepsilon_\infty^{-1}\omega^2\tau_M^2}{1+\omega^2\tau_M^2} \tag{15}$$

$$M''_D = \frac{(\Delta\varepsilon/\varepsilon_S\varepsilon_\infty)\omega\tau_M}{1+\omega^2\tau_M^2} \tag{16}$$

where the relaxation time is given by:

$$\tau_M = \frac{\varepsilon_\infty}{\varepsilon_S}\tau \tag{17}$$

and the peak magnitude is

$$M''_{D\,max} = \frac{1}{2}\frac{\varepsilon_S - \varepsilon_\infty}{\varepsilon_S\varepsilon_\infty} \tag{18}$$

located at $\omega_{max} = \tau_M^{-1}$.

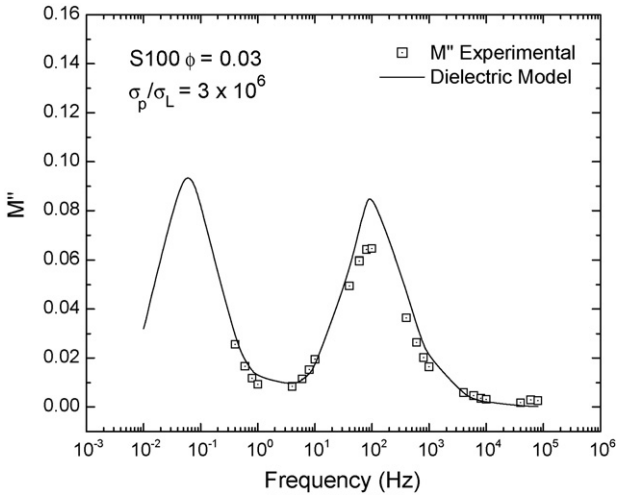

Fig. 2. Imaginary part of the dielectric modulus vs. frequency of silica particles in silicon oil. Predictions at low frequency follow Eq. (12), and those at moderate frequency follow Eq. (16). Particle volume fraction is 0.03. Values of the constants are: $\tau_M = 1.36E{-}3$ and $\tau_{MC} = 2.76$.

The values of the relative permittivity at low and high frequencies can be extracted from Fig. 1b, i.e., $\varepsilon_S = 5.25$ and $\varepsilon_\infty = 2.7$. By Eq. (17), the modulus peak is shifted to higher frequency (around 100 Hz) than that of the Debye peak shown in Fig. 1a, since $\tau_M < \tau$ (see Fig. 2). The value of the maximum according to Eq. (18) is 0.078. The conductivity peak in Fig. 2 is located at a frequency calculated from Eq. (13) (around 0.06 Hz). The magnitude of the maximum calculated from Eq. (14) is 0.10.

For increasing concentration ($\phi = 0.16$) the suspension with silicon oil (Fig. 3a and b) shows an increase in the static and optical permittivities and a decrease in the relaxation time, manifested as a shifting of the Debye peak to higher frequencies (200 Hz) as shown in Fig. 3a. The conductive part of the dielectric loss varies inversely with frequency, as the interfacial polarization mechanism predicts, although at this concentration the slope has a lower value. However, it is possible to find an approximate value of the characteristic time of the conductive part of these data from Eq. (6) in the limit of low frequency. Data shown in Fig. 3b reveal that the values of the permittivities are approximately $\varepsilon_S = 8.5$ and $\varepsilon_\infty = 3$. The conductive peak of the modulus spectrum, as shown in Fig. 4, is located at a frequency of 0.12 Hz with magnitude of 0.066, according to Eqs. (13) and (14). The Debye peak is located at 765 Hz with magnitude of 0.10, according to Eqs. (17) and (18). The conductive contribution to the spectrum has a characteristic frequency that increases with concentration and the relaxation part of the spectrum has a characteristic frequency that also increases with rising particle concentration.

Modeling of the more conductive systems, i.e., silica particles with either DOP or TCP, requires consideration to a non-localized conduction process [11] in which $\varepsilon_S \to \infty$, $\tau_\varepsilon \to \infty$ and $\varepsilon_\infty = C/C_0$ (C_0 is the vacuum capacitance). Non-localized conduction is a diffusion process in which the conductivity relaxation time, instead of the Debye relaxation time, is the characteristic variable of the process. In fact, this non-localized

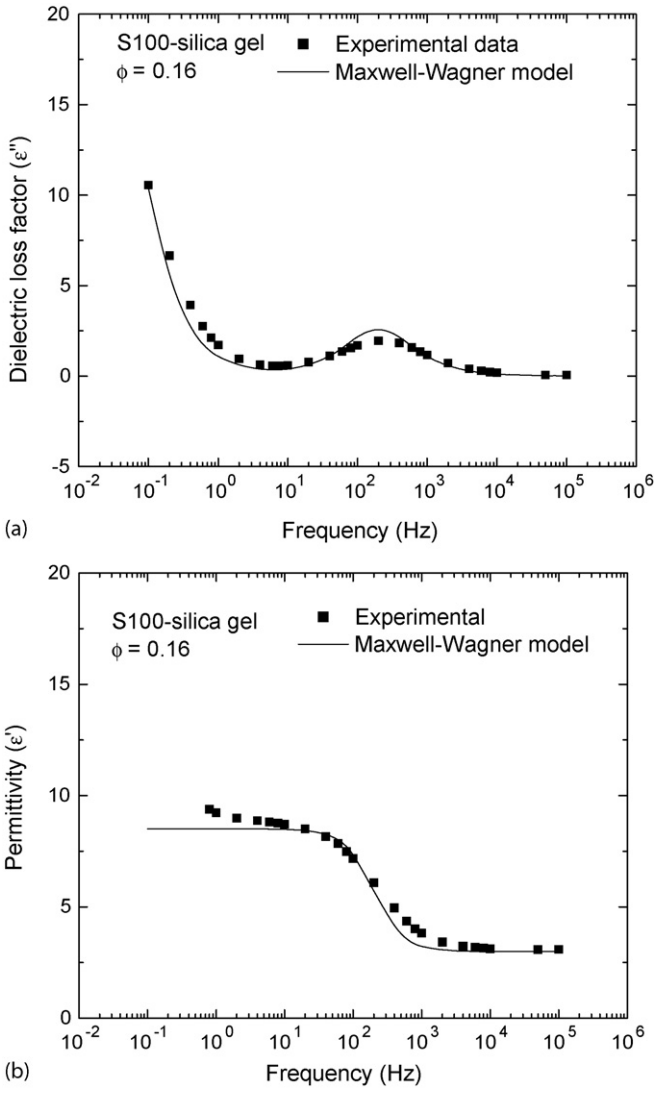

Fig. 3. (a) Dielectric loss and (b) relative permittivity, vs. frequency of silica particles in silicon oil. Experimental data and predictions of the Maxwell–Wagner polarization model (Eqs. (6) and (7)). Particle volume fraction is 0.16. Values of $\varepsilon_\infty = 3.0$, $\varepsilon_S = 8.5$, $\tau_1 = 4.8E{-}4$, $\tau_2 = 310$ and $\tau_w = 0.46$.

process can be regarded as a localized one with an infinitely long time constant, and then, it can be related to the Debye relaxation with some restrictions. Therefore, the ideal conduction or non-localized conduction can be treated as a extremely strong Debye relaxation, with high dielectric loss usually accompanied by rising ε' at low frequency. In the absence of interfacial effects, the non-localized conductivity is known as the dc conductivity. This leads to the result that the relaxation times of the modulus and impedance are almost equal. Here we use the impedance representation of data since in this case a semicircle will now appear in the complex impedance plane rather than in the dielectric constant plane. The expressions for the real and imaginary parts of the modulus and impedance spectrum are given by:

$$M' = \frac{\varepsilon_\infty^{-1}\omega^2\tau_M^2}{1+\omega^2\tau_M^2} \tag{19}$$

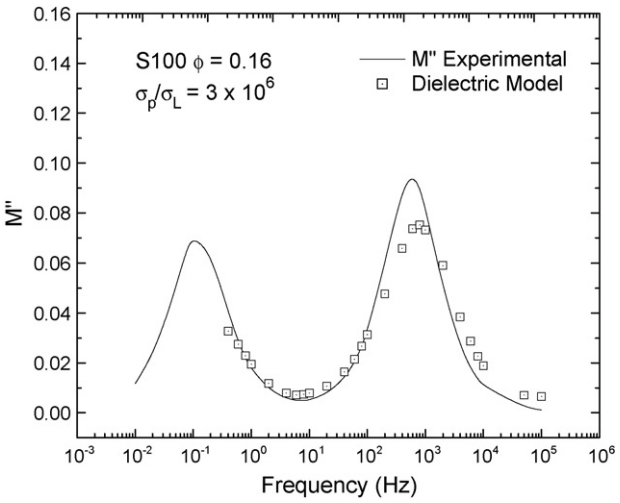

Fig. 4. Imaginary part of the dielectric modulus vs. frequency of silica particles in silicon oil. Predictions at low frequency follow Eq. (12), and those at moderate frequency follow Eq. (16). Particle volume fraction is 0.16. Values of the constants are: $\tau_M = 2.0E{-}4$ and $\tau_{MC} = 1.3$.

$$M'' = \frac{\varepsilon_\infty^{-1}\omega\tau_M}{1+\omega^2\tau_M^2} \tag{20}$$

$$Z' = \frac{R}{1+\omega^2\tau_Z^2} \tag{21}$$

$$Z'' = \frac{R\omega\tau_Z}{1+\omega^2\tau_Z^2} \tag{22}$$

Eqs. (21) and (22) can be represented by an equivalent RC circuit used to describe polycrystalline electrolytes [12].

When the DOP is used as dispersant, the ratio of particle conductivity to liquid conductivity is 87. At low particle concentration (0.03), M'' presents two peaks with different magnitude (Fig. 5) but smaller that those obtained using S100, indicating that the relative permittivity of this system is larger. The

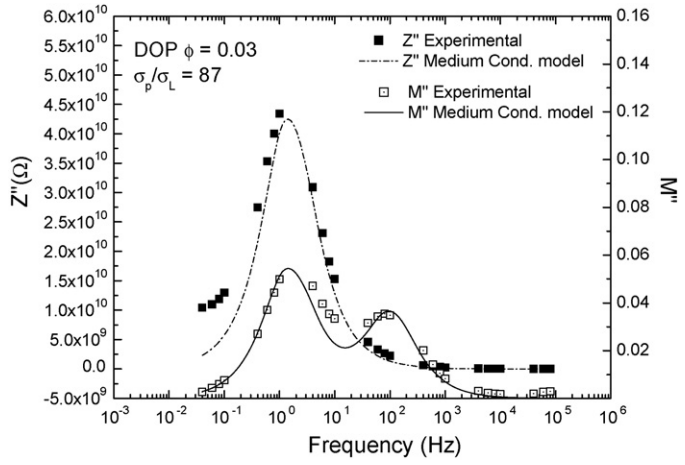

Fig. 5. Imaginary part of the impedance and modulus vs. frequency of silica particles in dioctyl phthalate (DOP). Particle volume fraction is 0.03. Experimental data and predictions from Eqs. (16) and (20) (modulus) and (22) (impedance) are shown.

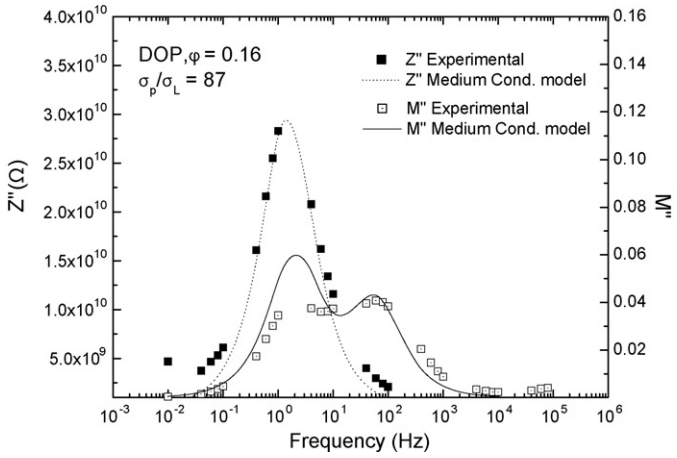

Fig. 6. Imaginary part of the impedance and modulus vs. frequency of silica particles in dioctyl phthalate (DOP). Particle volume fraction is 0.16. Experimental data and predictions from Eqs. (16) and (20) (modulus) and (22) (impedance) are shown.

impedance peak is located at the same frequency of the first modulus peak (1 Hz), because the modulus and impedance relaxation times are equal. The second modulus peak is located at a frequency around 100 Hz. Similar behavior has been reported for polycrystalline electrolytes [12], having two phases with different relative permittivity and conductivity. As described before, in the impedance representation, the impedance peak corresponds to dominating resistance of the system, i.e., the resistance at the liquid–particle interface. Because the impedance peak is located in the low frequency range of the spectrum, it is likely that this peak is related to the interfacial resistance at the liquid–particle interface. The higher frequency modulus peak may represent the bulk conductive structure with lower resistance than that of the interface.

When the concentration of particles increases (Fig. 6), the position of the peaks is similar to that at lower concentration, but with small increment in magnitude in (M'', Z''). The interfacial conductivity is larger but the bulk conductive structure remains with no substantial change.

With TCP, the particle and liquid conductivity are almost equal, and the behavior of M'' and Z'' at low (0.03) and high (0.16) particle concentrations is shown in Figs. 7 and 8, respectively. For $\phi = 0.03$, the two peaks in M'' tend to merge. The first one corresponds to the interfacial resistance and has a similar characteristic frequency of the impedance peak. Notice that both the impedance and modulus peaks appear now at a frequency of 100–200 Hz, a frequency shift of two decades from that with DOP. As compared with the DOP system, in this case the interfacial resistance is much lower (more than two decades), and the tendency to merge of the modulus peaks reflects that the particle and liquid phases tend to become a single conductive phase. As the particle concentration increases to $\phi = 0.16$, the overall behavior does not change substantially, although the resistance increases. The difference between the impedance and modulus relaxation times becomes less significant when the permittivities of particle and liquid are similar, as demonstrated by Hodge et al. [12]. The process shown here corresponds to a non-localized

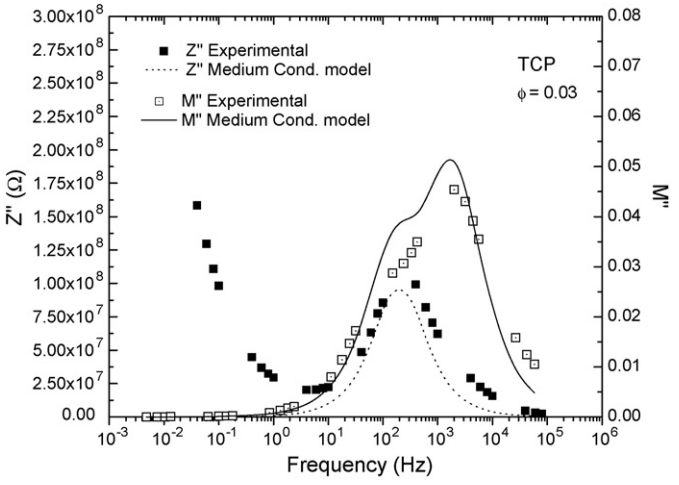

Fig. 7. Imaginary part of the impedance and modulus vs. frequency of silica particles in tricresyl phosphate (TCP). Particle volume fraction is 0.03. Experimental data and predictions from Eqs. (16) and (20) (modulus) and (22) (impedance) are shown.

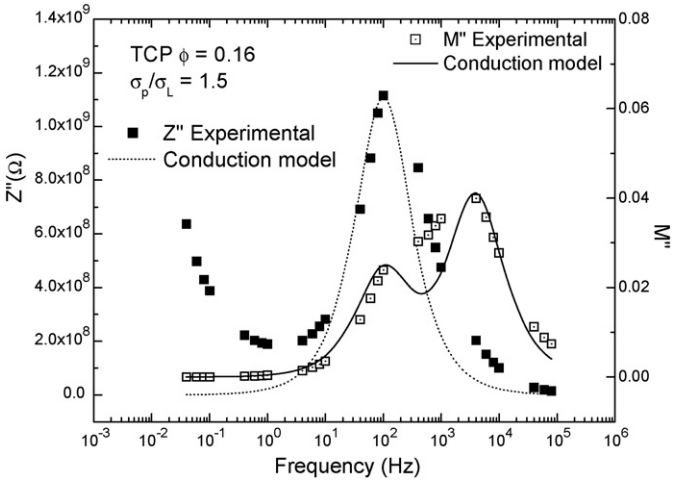

Fig. 8. Imaginary part of the impedance and modulus vs. frequency of silica particles in tricresyl phosphate (TCP). Particle volume fraction is 0.16. Experimental data and predictions from Eqs. (16) and (20) (modulus) and (22) (impedance) are shown.

conduction mechanism or long-range diffusion process and the suspension acts as a single phase. This occurs in the pure liquid or at high particle concentration. The spikes showed in the impedance spectra in Figs. 7 and 8 correspond to the electrode effects, which are separated from the bulk response and moved down the frequency scale. These spikes observed in the Z'' spectrum of the TCP suspension may be ascribed to high impedance due to the generation of charge carriers at the metallic–liquid interface, resulting from electrochemical reactions [13]. These effects are invisible in the modulus spectrum, since the electrode relative permittivity attains very high values, as explained before.

4. Conclusions

The dielectric spectrum of particle suspensions of different conductivity was analyzed with the Maxwell–Wagner polarization and Debye models. The dielectric spectrum of dilute suspensions of low conductivity reveals a Maxwell–Wagner interfacial polarization dominated by the conductive term at low frequencies, where the dielectric loss has a slope of minus one. A Debye peak is observed at moderate frequency. In the modulus representation, the presence of the two peaks, a conductive and a relaxation peak, is clearly observed. As the concentration increases, the slope in the conductive regime of the dielectric loss lowers, but the relaxation peak remains the same.

As the conductivity of the suspension increases, the dielectric spectrum is dominated by a delocalized diffusion process of the charges, which is modeled with expressions for the dielectric spectra similar to those reported for polydomain electrolytes. The interfacial resistance decreases substantially as revealed by the tendency of the modulus peaks to merge, which reflects that the particle and liquid phases tend to become a single conductive phase.

The dielectric behavior of suspensions with different conductivity largely influences the electrorheological response of the systems. In fact, with increasing conductivity, the variation of the viscosity and yield stress of the suspension with electric field changes. It is quadratic at low electric fields or low particle concentrations, but becomes less dependent of the electric field due to decreased particle polarization brought about by higher conductivity. This aspect is examined in detail in Part 2.

Acknowledgements

Financial support from CONACYT project 31123-U and IIE project 11794 are gratefully acknowledged.

References

[1] A. Gast, C. Zukoski, Adv. Coll. Int. Sci. 30 (1989) 153.
[2] L.C. Davis, J. Appl. Phys. 73 (1993) 680.
[3] T. Hao, A. Kawai, F. Ikasaki, Langmuir 14 (1998) 1256–1262.
[4] T. Hao, A. Kawai, F. Ikasaki, Colloid Interf. Sci. 239 (2001) 106–112.
[5] M. Pathasarathy, D.J. Klingenberg, Mater. Sci. Eng. R17 (2) (1996) 57–103.
[6] A. Kawai, et al., J. Chem. Phys. 109 (1998) 4587–4591.
[7] H. BlocK, J.P. Kelly, A. Qin, T. Watson, Langmuir 6 (1990) 6–14.
[8] H. BlocK, P. Rattray, T. Watson, Proceedings of the 3rd International Conference on ERF, 1992, p. 93.
[9] L. Marshall, F. Zukoski, J.W. Goodwin, Effect of electric field on the rheology of non-aqueous concentrated suspensions, J. Chem. Soc. Faraday Trans. 85 (1989) 2785–2795.
[10] K.D. Weiss, J.D. Carlson, Int. J. Mod. Phys. B 6 (15 and 16) (1992) 2609–2623.
[11] R. Gerhardt, W. Cao, Solid State Ionics 42 (1990) 213–221.
[12] I.M. Hodge, M.D. Ingram, A.R. West, J. Electroanal. Chem. 74 (1976) 125–143.
[13] A. Castellanos, Coulomb-driven convection in electrohydrodynamics, IEEE Trans. Electr. Insul. 26 (6) (1991) 1202–1215.